An Experimental Study on the Visual Detection of Stars in a Spacecraft Environment

R. P. HEINISCH*
Honeywell Inc., St. Paul, Minn.

Astronauts have experienced difficulty in seeing navigational stars through spacecraft windows on the illuminated side of the spacecraft. The objective of this investigation was to predict the star magnitude which can be seen with the naked eye or a sextant telescope through a spacecraft window. The effects of geometry and window coating are included. Scattering luminance of typical spacecraft windows was measured. Window illumination from the sun, moon, and Earth were computed for typical orbit conditions. Stellar magnitude thresholds were predicted from the scattering data and window illuminations by applying the classical Tiffany visual threshold data. The stellar thresholds indicate that window cleanliness is of paramount importance in reducing light scattering. Scattering measurements reveal that quality of the antireflection coating on windows has more influence on the scattering level than the type of coating per se. The better windows had a scattering level as low as a highly polished optical flat. Painting the edges of the window black reduced the light scattering. Light scattering created by multiple-window configurations was found to be equivalent to the sum of individual windows. The stellar magnitude thresholds are given for the telescope and the naked eye at the location of maximum, minimum, and average scatter. In general, using a telescope, an astronaut in a spacecraft that is distant from the Earth or moon will be able to see stars less bright than a magnitude of 2.00. On the other hand, with the naked eye, an astronaut will have difficulty seeing the usual navigational stars under background conditions created by the light scattered from windows used in this program.

Nomenclature

E, E_λ = illuminance and spectral illuminance, respectively
$E_{\lambda_{max}}$ = maximum spectral illuminance
E_0 = incident illumination on window
L_B = background luminance
L_W = luminance measured from window
L_d = luminance on diffuser
m_t = star magnitude
M = optical magnification
n = window normal
V_λ = relative spectral response of the eye
ψ = angle between incident beam and window normal
θ = angle between detector and window normal
ρ = reflectance
τ = transmission

Introduction

THERE is relatively little information available in the open literature describing scattering from transmitting elements. Munis and Finkel[1] have examined the scatter of infrared energy from Irtran materials.

The visibility of stars and planets during twilight has been treated comprehensively by Tousey and Koomen.[2] The optical environment for the Gemini flights has been examined by Ney and Huch.[3] They include the results of an experiment performed on a Gemini flight. The dominant source of stray light is the sun; most authors including the present use the Johnson[4] solar spectrum for their computations.

One of the more comprehensive sources of information on in-flight experiments is Ref. 5. A description of the rendezvous techniques, procedures, and flight data charts developed for the Gemini VI-A are presented by Stafford, Shirra, and Grim.[5] Roach, Dunkleman, Gill, and Mercer[5] have tabulated various general features obtained through visual observations by astronauts. Stars sightings are discussed in some detail by the latter authors.

Three probable causes for difficulties experienced by astronauts in seeing stars through spacecraft windows have been suggested. These causes are: a cloud of debris (dumped waste, spacecraft outgassants, and reaction jet exhausts) surrounds the craft; the windows become contaminated with condensates and vehicle outgassants which both reduce transmission and cause increased light scattering in the field of view; the clean window itself scatters and reflects light from other sources, such as the sun, which creates a luminous veil.

The purpose of this investigation was to study this last effect by completing the following tasks: measuring the light-scattering of various window orientations; calculating the light incident on the window for each specified "source" (sun, moon, and Earth); generating a stellar threshold model from the existing vision literature; calculating star magnitude thresholds (the ability of an astronaut to see stars is the minimum stellar magnitude that can be detected through a window).

The scattered light distribution of six window configurations was measured with the simulated solar spectrum incident at specified angles. The window configurations contain various combinations of MgF_2-coated, HEA†-coated, and uncoated Vycor window panes. The results were used to compute the minimum star intensity that can be seen with the naked eye and a monocular telescope through the window for various viewing angles.

Received August 8, 1970; revision received March 8, 1971. Work performed for NASA Ames Research Center on Contract NAS 2-5015. Also, the author wishes to acknowledge the contributions of C. L. Jolliffe, R. N. Schmidt, E. A. Bursch, and C. L. Tien.

* Principal Research Scientist.

†HEA refers to high efficiency antireflection coatings which are a proprietary product of Optical Coatings Laboratory Inc.

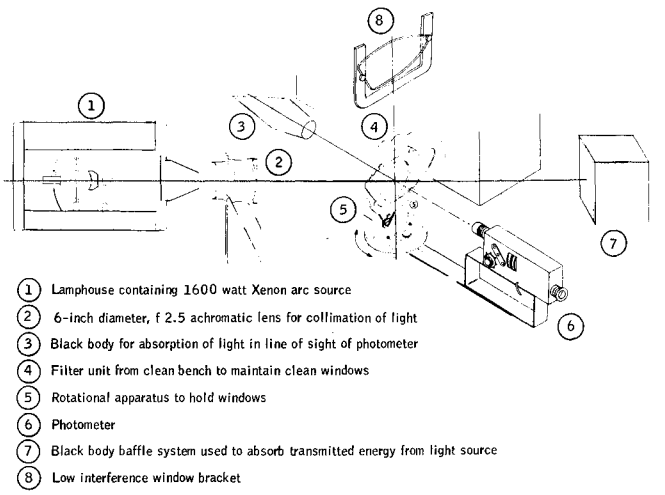

Fig. 1 Schematic of experimental apparatus.

Experimental Measurement Apparatus and Procedures

To predict star magnitudes visible through spacecraft windows on the illuminated side of space vehicles, it is necessary to know the scattering luminance from the windows. Because such information was not available, an experimental determination was necessary.

A schematic view of the test apparatus is shown in Fig. 1. Light from the lamphouse (1) originates from a defining aperture which is located at the focal point of a 6-in.-diam collimating lens (2), producing a (nominally) 6-in.-diam light beam incident on the window (5). Light scattered in various directions in a horizontal plane is recorded by a photometer (6). The background in the field of view of the photometer is darkened by placing a blackbody (3) on the optical axis of the photometer as shown. Light that is not reflected or scattered from the window is transmitted. The transmitted light is absorbed by a blackbody baffle system (7) which is located on the optical axis of the lamphouse-lens-window system. A filter unit (4) is used to blow filtered air over the window during the experiment to keep the window relatively free of dust.

The sun's spectrum has simulated with a xenon arc lamp, filter, and achromatic collimating lens. The light source was a 1600-w xenon arc lamp which produced a flux of 75,000 lumens. The energy distribution of the lamp in the visible was corrected with a Corning C5900 filter. To produce accurate collimation, a 0.125-in. aperture at the lamphouse exit was used to approximate a point of source. With the f2.5, 6-in.-diam, achromatic collimating lens, $\frac{1}{2}$ deg collimation was easily achieved.

The visible spectrum of the light beam incident on the window is shown in Fig. 2 along with published data on the sun's spectrum. In the spectral interval of 400 to 475 mμ, the sensitivity of the eye is so small that the source variance from the sun in that region is negligible. To illustrate, Fig. 3

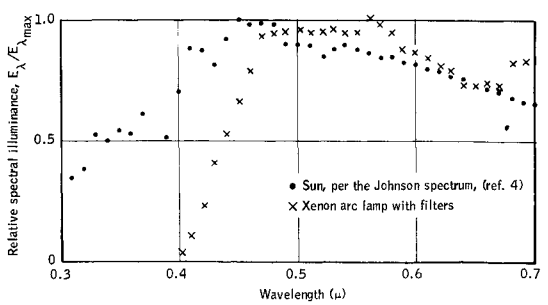

Fig. 2 Comparison of lamp and sun spectra.

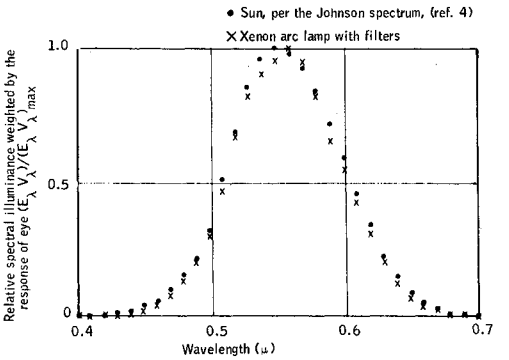

Fig. 3 Comparison of lamp and sun spectra weighted by eye response.

shows the spectral distribution of the source and sun weighted with the response of the eye, which reduces the deviations to small values.

The uniformity of the beam shown in Fig. 4 is within a 10% deviation across the 4 in. region of the horizontal plane from which the light incident on the photometer is scattered. The window was mounted to allow angular motion about two axes. The first rotation was about the window normal to study light scattering uniformity and the second rotation about a perpendicular to the window normal to vary the incident light angle.

A Pritchard photometer was used to make the scattering measurements and to determine incident illuminance. This particular instrument was chosen because 1) the manufacturer's stated accuracy is ±13% of full-scale reading over 13 orders of magnitude sensitivity; 2) the acceptance angle of the photometer could be varied; 3) it has internal calibration; 4) the instrument has a built-in filter so that the spectral response of the "standard eye" is modeled as shown in Fig. 5; and 5) it has an optical system which permits a visual check of the field of view.

The photometer was mounted on a movable arm so it could be rotated about the window while focused on the same spot on the window as seen in Fig. 1.

The window was initially aligned with an autocollimator to ensure that, at $\psi = 0$ (see Fig. 6), the front surface of the window was perpendicular to the incident light beam. This alignment was easily re-established during the course of the experiment by superimposing the image of the lamphouse aperture reflected from the front surface of the window on the aperture itself.

Because the window specimens were of finite size, the window edges were exposed to the incident light beam at incidence angles greater than 40°. The window edge, when illuminated, became a diffuse-like source of illumination that exceeded the luminance level of the measured field by about 2 orders of magnitude, necessitating further baffling of the photometer. To reduce stray light pickup by the photometer, a commercial light baffle with a $1\frac{1}{4}$-in.-diam aperture was attached to the Pritchard photometer.

Calibration with a photometer viewing a 100-ft Lambert standard source indicated that this light baffle with aperture did not occlude light from the photometer's viewing area, but it did reduce the background light effects.

To evaluate the effect of the window edge characteristics, several supplementary tests were run. It was determined

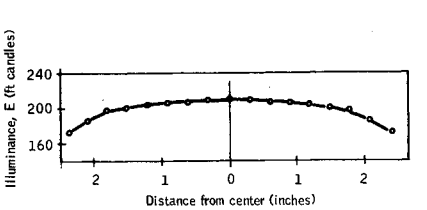

Fig. 4 Horizontal uniformity of beam.

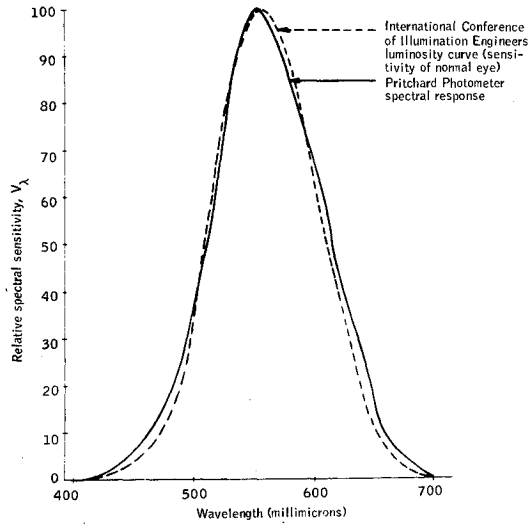

Fig. 5 Comparison of spectral response of eye and filter used on photometer.

that painting the edge reduced the light scatter levels. Because the edges of the windows used in this investigation were not highly polished they could have been a source of scattered light. This possible source could be reduced by polishing.

The window samples used in this investigation were supplied by NASA. They were space vehicle windows which were repolished and recoated commercially. The glass was Corning Vycor, and it was either uncoated, magnesium-fluoride (MgF_2) coated or high-efficiency, antireflection (HEA) coated. The windows were assigned a numerical designation shown in Table 1. This numerical identification is used throughout his paper.

The illumination incident on the windows was determined by two independent measurements. A photometer was used in the path of the light beam, while the Pritchard photometer was used to measure the light reflected from a diffuse disk placed in the light beam. The Gamma measurement was more direct but necessitated removing the window to make a measurement close to the window position. The Pritchard photometer, on the other hand, was used for the scattering measurements and a small diffuser disk could be placed directly in front of the window for routine illumination checks.

The Gamma photometer was calibrated with the Gamma standard light source. A series of five individual measurements was made of the incident illumination with photometer calibrations before each measurement. Table 2 is a sample of these individual measurements.

Measurement of the reflectance of the standard $BaSO_4$ disk nearly simultaneously with the scattering measurements permitted monitoring of incident illumination throughout the scattering measurements without removal of the sample win-

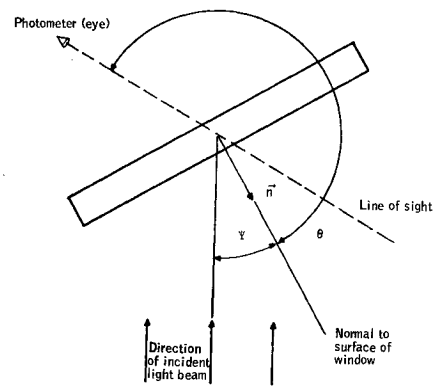

Fig. 6 Definition of angles used.

Table 1 Window identification

Number	Coating
208	MgF_2
240	Uncoated
244	HEA
246	HEA

dow or use of the Gamma photometer. Calibration of the photometer was performed according to National Bureau of Standards (NBS) procedures. An NBS standard lamp was use to illuminate a magnesium oxide target. The luminance was measured and compared to the NBS value. The internal standard was recalibrated to provide an accurate accessible calibration of the instrument during the experiments.

The last premeasuring task was reserved for cleaning of the sample windows. Normally, the windows are cleaned while mounted in the platform window mount with the intense collimated beam flooding the entire window. Under these illumination conditions, window surfaces frequently revealed surface film or particles that were unnoticed when they were cleaned and inspected under diffuse room illumination. Consequently, all windows received a final cleaning and visual inspection while positioned in the collimated beam.

Experience has shown that ultra-low scattering optical elements can be realized only if good cleaning practices are combined with a means of evaluating the effectiveness of cleaning.

The windows were cleaned using the following procedure. 1) Soak the element for several hours in hot "MICRO" detergent solution. 2) Rinse and rub with cotton swab while submerged in solution using deionized filtered water. Repeat this several times. 3) In a final step, the optical surface is covered with distilled deionized water which is blown off with a jet of dry nitrogen. The removal of the water should be complete. Also, care should be taken not to permit water droplets from the edge to flow across the optical surface after it is dry. 4) Inspect the cleaned surface by directing a bright collimated beam of light on the surface and viewing the surface against a black background in a darkened room. 5) If step 4 shows the optical element to be clean, proceed to measure scattering levels.

It is a general observation that a carefully cleaned optical surface usually does not become contaminated as readily as a poorly cleaned surface when exposed to normal laboratory environment.

Prediction of Star Magnitude Visual Thresholds

People with normal vision observing under normally clear atmospheric conditions are able to detect stars up to about the 6th magnitude. This three-fold range may be extended to the 7th magnitude when viewing where haze and extraneous light factors are significantly reduced. Though many factors are related to optimal viewing conditions, we can define four general factors that play a large role in the detection of a specific star: 1) the viewer's adaptation level; 2) the star's illuminance level in the plane of the viewer's eye; 3) background luminance level; and 4) the viewer's knowledge of star location. For our purpose, we have made two assumptions

Table 2 Incident illumination values as measured in the plane of the sample window

Measurement	Individual measurement, fc
1	178
2	181
3	175
4	177
5	180
	$\bar{E}_0 = 178.2$

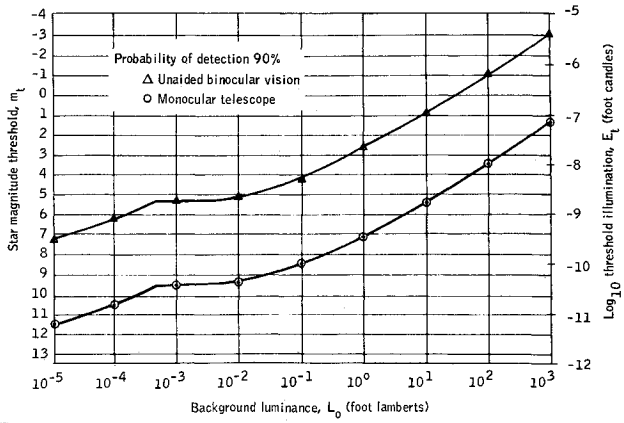

Fig. 7 Star magnitude detection threshold vs background luminance (in space).

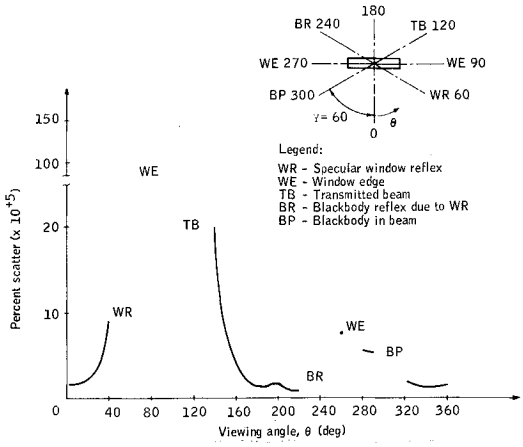

Fig. 9 Scatter distributions for window 240, $\psi = 60°$.

regarding these four factors: 1) the viewer's adaptation level corresponds to the existing luminance level; and 2) the viewer is knowledgeable concerning the star's location. The acceptance of these two assumptions greatly simplifies our star threshold prediction task and, in addition, permits us to draw on some available probability-of-detection data to supplement our detection threshold values.

Stellar magnitude, as established, is based on sea level illuminance levels. Consequently, to predict star magnitude threshold values from spacecraft it is necessary to correct stellar magnitude values for light losses due to atmospheric absorption and scatter. Baker[6] has equated this factor to a 30% increase in illumination at the edge of the atmosphere. This value converted to star magnitude extends the magnitude range by a factor of 0.22.

Figure 7 was plotted to serve as our stellar prediction threshold model from Hardy's[7] modification of Blackwell's Tiffany study.[8] On the right hand ordinate an illumination scale has been included which permits the reader to relate a threshold value to a corresponding illumination value (E). All values have been corrected to read star magnitude thresholds for the 90% probability of detection level and for exo-atmospheric viewing conditions.

We have generated a stellar magnitude threshold curve that corresponds to a sextant telescope with a 32 mm objective lens, a 4 mm exit pupil, a magnification factor (m) of 8× and a light transmittance factor (τ) of 0.65. We have based our set of telescope threshold values on the premise that illumination from the background is decreased by the transmittance factor 0.65 and that illumination from a star is increased by the numerical factor 41.6. The factor 41.6 is arrived at by calculating the product $M^2\tau$ or by the more accepted method of multiplying the transmittance factor times the square of the ratio of the objective lens to the exit pupil.

In practice, our model has some evident shortcomings. Regarding the reduction in background luminance level when viewing with or without the telescope, it is not likely that the viewing field will be devoid of other stars. Stars in close proximity to the viewing star will obviously contribute to light adaptation and then raise the visual threshold. In addition, we have assumed instant dark adaptation when in reality it is a rather slow process and therefore the assumption of complete adaptation is only partially correct for this case.

Scatter Measurements

Figures 8–10 illustrate the scattering distributions at the particular window incident orientation (ψ angles) where the minimum scattering occurs for windows 208, 240, and 246. The discontinuous character of the data would indicate few anomalous inputs during the course of the experiment.

The discontinuities evident in Figs. 8–10 are due to physical constraints inherent in the measurement apparatus and the physics of the problem. In particular, referring to Fig. 8, WR denotes the specular reflection from the window. As the window-sun angle increases (i.e., $\psi > 0°$) the specular reflection from the window is incident on the photometer at larger θ values. Although a valid measurement can (and was) be made at this position, the data from a scattering standpoint is anomalous. Also when the photometer is rotated to $\theta = 90°$ or 270° WE, the line of sight is parallel with the front and back surfaces of the window. In effect, the measurement is of the background only. The notation TB refers to the transmitted beam. The intense 6-in.-diam beam is, to a large extent, transmitted by the window(s). Again, measurements could have been made but they would have indicated the transmittance of the window and not the scattering in a par-

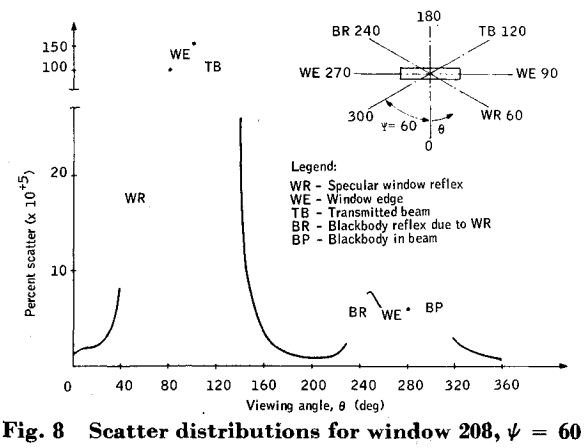

Fig. 8 Scatter distributions for window 208, $\psi = 60°$.

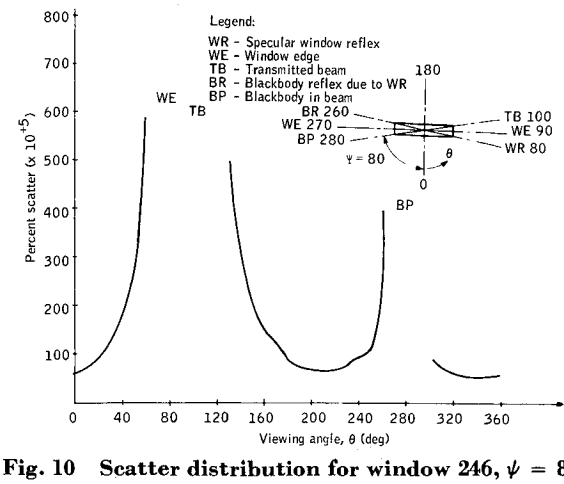

Fig. 10 Scatter distribution for window 246, $\psi = 80°$.

Table 3 Star magnitude predictions, sun at 1 a.u.

Mode of observation	Veiling luminance: No internal reflection: Window 208	Window 240	Window 244	Window 246	Window 244 & 208	Window 244 & 246	With internal reflection: Window 208		Window 208 & 246	
Maximum	$\psi = 60°$ $\theta = 100°$	$\psi = 60°$ $\theta = 100°$	$\psi = 60°$ $\theta = 100°$	$\psi = 50°$ $\theta = 100°$	$\psi = 50°$ $\theta = 100°$	$\psi = 60°$ $\theta = 100°$	$\psi = 80°$ $\theta = 0°$		$\psi = 80°$ $\theta = 0°$	
Telescope	5.50	5.50	5.50	3.70	3.50	3.30	3.60[a]	2.75[b]	2.75[a]	2.00[b]
Eye	1.00	1.00	1.00	−0.75	−1.00	−1.15	−0.95	−1.75	−1.75	−3.20
Minimum	$\psi = 80°$ $\theta = 200°$	$\psi = 10°$ $\theta = 100°$	$\psi = 80°$ $\theta = 220°$	$\psi = 80°$ $\theta = 210°$	$\psi = 80°$ $\theta = 210°$	$\psi = 60°$ $\theta = 220°$	$\psi = 0°$ $\theta = 100°$		$\psi = 0°$ $\theta = 100°$	
Telescope	8.75	8.05	9.50	6.50	8.25	6.75	5.65	4.75	4.75	5.50
Eye	4.50	3.80	5.25	2.25	4.00	2.35	1.10	0.35	0.35	1.10
Average										
Telescope	6.00	6.00	6.00	4.25	4.00	3.80	4.25	3.05	3.00	3.45
Eye	1.50	1.70	1.50	−0.25	−0.25	−0.45	−0.25	−1.40	−1.50	−0.65

[a] Reflection off astronaut helmet.
[b] Spacecraft internal reflection (9 ft diam).

ticular direction. When the photometer is rotated such that the blackbody is flooded by the transmitted beam, the photometer views a background (the illuminated blackbody) that is of higher intensity than the scattering per se. Consequently, measurements could not be made at this position. In like manner, the blackbody cannot be placed directly in the path of the light beam which is specularly reflected from the window. This instance is denoted BR.

Of particular interest is a direct comparison of Figs. 8 and 9. These curves include the locations where the lowest scattering value occurs for windows 208 (MgF_2) and 240 (uncoated). The two scattering distributions are quite similar. This likeness is remarkable in light of the differences in the two windows. Equally surprising is the fact that the maximum values for scattering occur at the same viewing angle (θ) as well as the same angle of incidence (ψ). Other similarities were also evident in the bulk of the scattering data.

The scattering distribution for window 246 (HEA) is presented in Fig. 10. Scattering values are obtained for this window that are an order of magnitude greater than for all other windows. The increased scattering appears to be due to the surface coating. The mechanism in the surface coating causing the light scatter is unknown. The coating appeared, under intense illumination, to have a foggy opaque composition. The particular coating quality is extremely important.

Detection Thresholds

The data from the four windows and the two window combinations (244 and 208, 244 and 246) was used to make star magnitude threshold predictions based on the star magnitude prediction model proposed earlier in this paper for specific sources of luminance.

The sources under consideration were the sun, moon, Earth, and internally reflected energy within a spacecraft. The moon was approximated using an albedo of 0.07 times the solar spectra. The Earth was simulated using an albedo of 0.35 when it was at extreme distances from the Earth. For the situations where the Earth was close to the vehicle, a numerical scheme was developed to include the complex geometrical interrelationships involved. The Earth's surface was divided into 200 by 200 areas and the window illumination was divided into conical segments. The reflected energy within the vehicle was accounted for by assuming diffuse reflection from within a 6-ft-diam sphere with a 0.7 reflection coefficient.

The star magnitude threshold predictions are presented in Tables 3, 4, and 5. These star threshold values are presented for each window studied, illuminated by an external source of light and for window 208 and a 208 and 246 combination illuminated by the internal reflection of the transmitted light beam. It should be noted that experimental scattering measurements were not made on the 246 and 208 combination. Instead, the individual scattering contributions were numerically added. This procedure is justified subsequently.

The tables contain star threshold values for the maximum, the minimum, and the average scattering values measured for the windows specified. Specific values of ψ and θ are given for the maximum and minimum. The star threshold com-

Table 4 Star magnitude predictions, Earth at 200 km

Mode of observation	Veiling luminance: No internal reflection: Window 208	Window 240	Window 244	Window 246	Window 244 & 208	Window 244 & 246	With internal reflection: Window 208		Window 208 & 246	
Maximum	$\theta = 0°$	$\theta = 0°$	$\theta = 0°$	$\theta = 0°$	$\psi = 50°$ $\theta = 100°$	$\psi = 60°$ $\theta = 100°$	$\psi = 80°$ $\theta = 0°$		$\psi = 80°$ $\theta = 0°$	
Telescope	2.50	2.50	2.40	1.00	0.75	0.50	1.00[a]	0.00[b]	0.00[a]	−0.50[b]
Eye	−2.00	−2.00	−2.10	−3.75	−4.25	−4.60	−3.75	−4.95	−4.75	−5.25
Minimum	$\theta = 160°$	$\theta = 160°$	$\theta = 160°$	$\theta = 160°$	$\psi = 80°$ $\theta = 210°$	$\psi = 80°$ $\theta = 220°$	$\psi = 0°$ $\theta = 160°$		$\psi = 0°$ $\theta = 160°$	
Telescope	6.60	6.70	6.70	3.75	3.50	3.25	3.50	2.75	2.75	2.25
Eye	2.20	2.30	2.30	−1.30	−1.05	−0.80	−1.20	−1.40	−1.50	−2.10
Average										
Telescope	3.10	3.05	2.50	1.25	1.00	0.75	1.00	0.25	0.25	−0.25
Eye	−1.40	−1.30	−2.05	−3.25	−3.50	−3.75	−3.75	−4.25	−4.30	−4.75

[a] Reflection off astronaut helmet.
[b] Spacecraft internal reflection (9 ft diam).

Table 5 Star magnitude predictions, moon at 130 km

Mode of observation	Veiling luminance: No internal reflection: Window 208	Window 240	Window 244	Window 246	Window 244 & 208	Window 244 & 246	With internal reflection: Window 208		Window 208 & 246	
Maximum	$\theta = 0°$	$\theta = 0°$	$\theta = 0°$	$\theta = 0°$	$\psi = 50°$ $\theta = 100°$	$\psi = 60°$ $\theta = 100°$	$\psi = 80°$ $\theta = 0°$		$\psi = 80°$ $\theta = 0°$	
Telescope	4.10	6.15	4.10	2.25	1.90	1.70	1.85[a]	0.75[b]	0.95[a]	0.00[b]
Eye	0.25	1.75	−0.30	−2.20	−2.55	−2.75	−1.75	−3.75	−3.35	−4.50
Minimum	$\theta = 160°$	$\theta = 160°$	$\theta = 160°$	$\theta = 160°$	$\psi = 80°$ $\theta = 210°$	$\psi = 80°$ $\theta = 220°$	$\psi = 0°$ $\theta = 160°$		$\psi = 0°$ $\theta = 160°$	
Telescope	7.25	7.30	7.30	6.50	6.15	5.90	5.30	4.75	4.50	4.00
Eye	3.10	3.15	3.15	2.10	1.75	1.50	0.80	0.35	0.00	−0.50
Average										
Telescope	4.50	4.90	4.60	2.50	2.15	1.90	2.25	1.50	1.25	0.50
Eye	0.10	0.45	0.20	−2.30	−1.95	−2.10	−2.25	−3.05	−3.25	−4.00

[a] Reflection off astronaut helmet.
[b] Spacecraft internal reflection (9 ft diam).

putations are based on two modes of observations, i.e., the naked eye and the telescope. Maximum means the largest valid scattering value measured. Obviously, measurements made of the transmitted beam, the specular reflection, or of the blackbody in the transmitted beam would be greatest in magnitude. However, such measurements are not herein considered valid scattering measurements. For example, when $\psi = 0°$, the transmitted beam extends from θ of 165° to 195°. Therefore, the valid data points adjoining this segment are θ of 190° and 200°. Other anomalous data points are self evident. The minimum data point refers to the lowest valid scattering value measured; the average refers to an arithmetic average of the maximum and the minimum scattering for the window considered.

Table 6 Additive scattering of windows 208 and 244 compared with actual experimental data and theory, $\psi = 0°$

θ	$\frac{L_w - L_B}{E_0 \cos\psi} \times 10^{-5}$: Superposition summation	Theory[a]	Experiment
20	5.74	7.86	4.10
30	3.03	3.42	2.54
40	2.24	2.28	2.01
50	1.98	1.82	1.82
60	1.89	1.53	1.73
70	1.97	1.54	1.74
80	2.19	1.63	1.64
100	2.81	1.83	1.54
110	2.86	1.92	3.79
120	3.12	2.11	4.72
130	3.69	2.48	4.56
140	5.19	3.13	5.48
150	8.99	5.08	7.81
160	18.92	12.93	17.29
200	21.74	14.68	18.28
210	12.57	5.50	8.25
220	5.45	3.52	4.90
230	3.97	2.38	4.03
240	3.50	2.09	3.62
250	3.31	1.71	3.15
260	3.29	2.11	1.64
280	2.13	1.54	1.42
290	2.34	1.52	1.84
300	2.17	1.52	1.83
310	2.35	1.73	1.98
320	2.94	1.95	2.18
330	3.05	2.68	2.61
340	4.49	4.65	3.97

[a] Theory used data for two 208 windows.

In general, Tables 3, 4, and 5 indicate that, using a telescope, an astronaut in a spacecraft distant from the Earth or moon will be able to see stars less bright than a magnitude of 2.00. On the other hand, with the naked eye, an astronaut would have difficulty detecting the usual navigational stars under background conditions produced by the light scatter from windows studied in this program.

Table 6 contains comparisons of reduced scattering data for two-pane window configurations. In particular, scattering values are presented for various viewing angles (θ) that are obtained in three separate ways. First, the data is obtained experimentally, that is, by measuring the scatter levels of the two-window configurations. Secondly, the data is obtained using standard theory. This calculation is based on the assumption that both windows are composed of the same material. This assumption was satisfied when the scattering from the individual windows was comparable, as in the case of windows 208 and 244. Finally, the scatter levels are also obtained by superposing (adding) the individual scattering levels from the respective windows that comprise the two-window system. It is evident that superposition gives quite accurate predictions for the two-window systems. This result was unexpected in light of the complexity of the light-scattering process, but it may be extremely useful for application of this data to a practical spacecraft where five or six windows may be utilized in series and a rough idea of the scatter is desirable.

Conclusions

The results of this investigation produced several significant conclusions. By preferentially orienting the spacecraft to obtain optimum viewing conditions, the astronauts may be able to see navigational stars that otherwise would be undetectable. For practical navigational purposes, a telescope would be required to detect stars consistently. Star detection could be appreciably enhanced if the effects of internal cabin light could be minimized. Back reflections of internal light off the window greatly increase the star magnitude required for visual detection. Using a monocular telescope a star with a magnitude of 9.9 can be seen through a single window under test conditions. With the naked eye under the worst viewing conditions considered, only a star of magnitude 5.25 can be detected. The quality of the surface coating is of primary importance, while the type of coating appears to have little influence on the light-scatter levels. The effects of contamination are perhaps the most significant in influencing the light-scatter levels. Elimination of contamination reduces the scatter levels more than any other overt mechanism.

Superposition of scatter levels (adding) is valid to obtain scatter of multiple (two-pane) window arrays. The window edges should perhaps be polished. Painting of the window edge also reduces the light-scatter levels.

References

[1] Munis, R. H. and Finkel, M. W., "Goniometric Measurements of Infrared Transmitting Materials," *Applied Optics*, Vol. 7, 1968, p. 2001.

[2] Tousey, R. and Koomen, M. J., "The Visibility of Stars and Planets During Twilight," *Journal of the Optical Society of America*, Vol. 43, No. 3, 1953, pp. 177–183.

[3] Ney, E. P. and Huch, W. F., "Optical Environment in Gemini Space Flights," *Science*, Vol. 153, 1966, pp. 297–299.

[4] Johnson, F. S., "The Solar Constant," *Journal of Meteorology*, Vol. II, No. 6, Dec. 1954, pp. 431–439.

[5] *Gemini Midprogram Conference, Including Experimental Results*, NASA SP-121, Feb. 23–25, 1966, pp. 283–297 and pp. 315–323.

[6] Hardy, A. C., "How Large is a Point Source?" *Journal of the Optical Society of America*, Vol. 57, No. 1, Jan. 1967, pp. 44–47.

[7] Blackwell, R. H., "Contrast Thresholds of the Human Eye," *Journal of the Optical Society of America*, Vol. 36, No. 11, Nov. 1946, p. 624.

AUGUST 1971 J. SPACECRAFT VOL. 8, NO. 8

Trajectory Requirements for Comet Rendezvous

ALAN L. FRIEDLANDER,* JOHN C. NIEHOFF,† AND JOHN I. WATERS‡
IIT Research Institute, Chicago, Ill.

This paper presents a new look at spacecraft mission opportunities to the short-period comets in the time period 1975–1995. The objective is to identify the most promising rendezvous opportunities and flight modes from the standpoint of trajectory requirements and launch vehicle/payload capabilities. A "broad-brush" treatment of wide scope underlies the analysis. Selection criteria leading to 16 comet apparitions for study are described. The candidate flight modes include; 3-impulse ballistic transfers, Jupiter-gravity-assist transfers, solar-electric and nuclear-electric low-thrust transfers. Results show that the best early opportunities are Comets Encke/80, d'Arrest/82, and Kopff/83. Although these missions can be performed ballistically, solar-electric propulsion offers greatly improved performance. Practical accomplishment of the very difficult Halley rendezvous depends upon the development and availability of nuclear-electric propulsion by 1983.

Introduction

SPACECRAFT missions to the comets can play an important role in the total space exploration program. An improved knowledge of cometary bodies should contribute to our understanding of the dynamics and origin of the solar system. In particular, "in situ" scientific measurements can provide information on the comet nucleus and the distribution of particles and fields in the coma and tail regions. This type of data is extremely difficult if not impossible to obtain from Earth-based observations.

A number of earlier studies[1–4] have reported on periodic comets and their scientific exploration by means of spacecraft intercept missions. These studies have presented the scientific objectives, a compendium of existing cometary data, trajectory and sighting analysis, and a survey of suitable missions including payload selection and questions of mission constraints. Comet intercept or flyby missions are characterized by relatively low launch velocity requirements and short flight times, but very high approach velocities at the comet leaving little time for science experiments. Clearly, it is more opportune that the spacecraft match orbits with the comet and thus have many months to monitor the variations in physical activity as the comet approaches and passes through perihelion. The present paper considers the rendezvous mission mode which affords this opportunity for increased science value return.

Several previous and enlightening investigations of comet rendezvous have been reported in the literature.[5–8] The present study[9] expands upon earlier work in this area in terms of the scope of mission opportunities available and the comparison of candidate modes of flight for performing these missions. Specifically, the objective is to identify the most promising rendezvous missions and flight modes in the time period 1975–1995 from the standpoint of trajectory requirements and launch vehicle/payload capabilities. Both the ballistic and low-thrust flight modes with two variations on each are considered. Ballistic flights include 1) direct transfers utilizing three velocity impulses and 2) gravity-assist transfers via the planet Jupiter thus eliminating the midcourse propulsive impulse. The low-thrust propulsion mode includes application of 1) solar-electric powerplants and 2) nuclear-electric powerplants. Use of nuclear-electric spacecraft will be emphasized only for the very difficult but exciting rendezvous mission to Halley's Comet. All trajectories are optimized to give effectively a maximum payload (net spacecraft mass delivered) for a given flight time and launch vehicle selection. Emphasis is placed on the programed Titan class launch vehicle and flight times consistent with delivering a payload of about 450 kg. An additional constraint generally applied is that the rendezvous point occur in the region 0–200 days before comet perihelion.

Comet Orbits and Ballistic Intercepts

Comets may be classified into two general groups; the short-period comets having orbital periods less than 1000 years but more typically on the order of 5–10 years, and the

Presented as Paper 70-1072 at the AAS/AIAA Astrodynamics Conference, Santa Barbara, Calif., August 19–21, 1970; submitted September 17, 1970; revision received April 1971. This work has been performed for the Office of Planetary Programs, NASA Headquarters under Contract NASW-2023.

* Senior Engineer, Astro Sciences. Member AIAA.
† Senior Engineer, Astro Sciences. Associate Member AIAA.
‡ Research Engineer, Astro Sciences. Member AIAA.